land

MDPI

Article

Microbial Transformation of Polyethylene Terephthalate Microplastics by Wetland-Derived Microbial Communities: Implications for Coastal Sediment Systems

Jing Dong [1], Guo Li [1,2], Jiao Ran [1], Zhe Li [1], Shanyuan Xue [1], Dan Zhou [3], Weizhen Zhang [4,*] and Zheng Zheng [1,*]

[1] Department of Environmental Science and Engineering, Fudan University, Shanghai 200433, China; 23210740033@m.fudan.edu.cn (J.D.); guoli21@m.fudan.edu.cn (G.L.); 23110740048@m.fudan.edu.cn (J.R.); 24210740044@m.fudan.edu.cn (Z.L.); 23210740022@m.fudan.edu.cn (S.X.)
[2] MOE Key Laboratory for Biodiversity Science and Ecological Engineering, National Observations and Research Station for Wetland Ecosystems of the Yangtze Estuary, School of Life Sciences, Fudan University, Shanghai 200433, China
[3] Yancheng Tiaozini Wetland Research Institute Co., Ltd., Yancheng 224237, China; yujiantiaozini@126.com
[4] School of Ecological Environment, Chengdu University of Technology, Chengdu 610059, China
* Correspondence: zwz@cdut.edu.cn (W.Z.); zzhenghj@fudan.edu.cn (Z.Z.)

Abstract

Microplastics are persistent contaminants in coastal wetlands, yet the mechanisms of their microbial transformation remain poorly understood. This study examined the interactions between a wetland sediment-derived microbial consortium and polyethylene terephthalate (PET) fibers over a 60-day incubation. After 60 days, the consortium caused a PET weight loss of 13.7 ± 0.9%, whereas the abiotic control showed a less than 2% loss. The water contact angle decreased from 77.5 ± 1.2° to 75.8 ± 0.4°, suggesting enhanced surface hydrophilicity. Multi-scale surface analyses (SEM, WCA, and FTIR) confirmed progressive microbial colonization, increased surface roughness, and enhanced hydrophilicity through microbially mediated modification. High-throughput 16S rRNA sequencing unveiled a distinct community succession; PET exerted selective pressure that reduced alpha-diversity while enriching specific functional taxa such as *Acinetobacter* and *Pseudomonas*. Moreover, isolation and co-culture assays confirmed the importance of synergistic microbial interactions in PET transformation, with co-culture of four representative isolates causing 9.2 ± 0.1% PET weight loss, compared with only 1.7–3.2% in monocultures. These findings underscore the intrinsic natural attenuation potential of wetland ecosystems and provide a critical scientific basis for developing nature-based management strategies. By identifying key functional taxa and PET-associated transformation pathways, this work supports the establishment of early-warning mechanisms to safeguard the ecological integrity and soil health of coastal World Natural Heritage sites like the Tiaozini Wetland.

Keywords: community succession; microbe–plastic interactions; polyethylene terephthalate (PET); wetland sediments; land system resilience

Check for updates

Academic Editors: Nunziarita Palazzolo and Luca Furnari

Received: 9 February 2026
Revised: 13 March 2026
Accepted: 17 March 2026
Published: 19 March 2026

Copyright: © 2026 by the authors. Licensee MDPI, Basel, Switzerland. This article is an open access article distributed under the terms and conditions of the Creative Commons Attribution (CC BY) license.

1. Introduction

Plastic pollution, especially microplastics (MPs), has become a widespread environmental issue [1]. Their persistence, extensive distribution, and potential ecotoxicological impacts on both aquatic and terrestrial ecosystems have raised significant concerns [2,3]. Polyethylene terephthalate (PET) is one of the most frequently used synthetic polymers,

finding broad applications in packaging, textiles, and beverage containers [4,5]. Owing to its high crystallinity and hydrophobicity, PET is highly resistant to environmental transformation and tends to accumulate in sediments and biota. This is particularly evident in coastal and wetland environments, where hydrodynamic deposition and vegetation trapping enhance its retention [6,7].

Wetlands, functioning as transitional areas between terrestrial and marine ecosystems, not only act as repositories for MPs but also potentially serve as key sites for biogeochemical transformation [7]. While the fate and transport of MPs have been thoroughly investigated in marine and freshwater systems [8,9], research specifically targeting PET biodegradation within natural wetland ecosystems remains limited. Most existing studies have focused on the degradation capacities of isolated bacterial strains from landfills [10], composting systems [11], or wastewater treatment plants [12,13], under controlled laboratory conditions. However, these artificial settings differ significantly from wetland environments, where sediment microbial communities are shaped by tidal cycles, fluctuating redox conditions, and complex organic matter interactions.

Recent studies have begun to reveal the potential of wetland sediments as reservoirs of PET-degrading microbial consortia. For instance, Niu highlighted that dynamic redox conditions in tidal sediments foster microbial metabolic flexibility and plastic-degrading capacity [14,15]. Fang demonstrated a cooperative system involving aerobic *Pseudomonas* and anaerobic *Desulfopila* in mangrove sediments, where the former oxidized polyethylene using laccase under aerobic conditions, and the latter mineralized intermediates during anaerobic phases [16]. Similarly, *Acinetobacter venetianus* and *Bacillus albus* were shown to degrade polyethylene in a complementary manner, with surface modification by the former enhancing substrate availability for the latter under oxygen-limited conditions [17]. These findings suggest that functional complementarity and resource exchange among microbial taxa may drive efficient plastic degradation in natural sediments. Moreover, the interaction between MPs and microbial communities is not unidirectional. MPs can reshape microbial consortium structure by providing novel colonization niches which often harbor opportunistic pathogens and antibiotic resistance genes [18]. Environmental stressors such as sea level rise and salinity shifts may further exacerbate PET persistence and its long-term ecological impacts [19]. Therefore, understanding how native sediment microbial consortia adapt to and transform PET microplastics in wetland environments is of both ecological relevance and bioremediation significance.

Among the various mitigation strategies, microbial transformation offers a sustainable, low-energy solution. Numerous microorganisms have demonstrated plastic-degrading capabilities via enzymatic hydrolysis, radical oxidation, and biosurfactant-mediated pathways [20,21]. Notably, PETase-expressing strains like *Stenotrophomonas pavanii* have shown promise in enhancing PET-associated transformation [22]. Other bacteria such as *Microbacterium DEHP-1* can metabolize plasticizers through esterase and monooxygenase activity, fully mineralizing them to CO_2 [10,23]. However, most of these studies are based on monocultures, while the synergistic mechanisms, functional succession, and regulatory dynamics within complex microbial communities remain poorly understood.

Recent advances suggest that co-cultivation can enhance degradation efficiency. For example, *Bacillus–Enterobacter consortia* exhibited improved breakdown of algal-based plastics [24], and co-cultures of *Stenotrophomonas maltophilia* and *Bacillus velezensis* achieved over 40% degradation of polystyrene within 60 days [25]. Yet, such studies often lack in-depth analyses of community succession and microbial functional shifts during degradation.

Coastal wetlands represent critical land–sea transition zones that function as long-term sinks for microplastics transported from both terrestrial and marine sources [7]. Owing to high sedimentation rates and complex biogeochemical conditions, microplastics including

PET can accumulate and persist in wetland soils, where they may alter soil structure, microbial processes, and overall ecosystem functioning [18,19,26,27]. Understanding how indigenous microbial communities interact with and transform PET microplastics in wetland sediments is therefore not only relevant to plastic biogeochemical cycling, but also closely linked to land system stability, soil health, and the ecological integrity of coastal wetlands. This issue is particularly important for protected and sensitive land systems, such as the Tiaozini Wetland, a World Natural Heritage Site, where long-term microplastic accumulation may pose risks to sediment quality and ecosystem resilience.

In this study, we hypothesize that PET microplastics act as persistent solid substrates that reshape microbial community structure and induce co-metabolic surface modification. To examine this hypothesis, we investigated the interactions between PET microplastics and a sediment-derived microbial consortium enriched from the Tiaozini Wetland, located in the Yellow Sea region of eastern China. By integrating PET surface characterization, microbial community profiling, and functional pathway analysis, this work aims to (i) evaluate PET-associated transformation and mass loss mediated by the microbial consortium, (ii) identify key microbial taxa associated with different transformation stages, and (iii) explore the role of community succession and co-metabolic interactions in regulating PET transformation under wetland-simulated conditions. Unlike studies focusing on isolated strains, this work emphasizes the ecological relevance of community-level processes in PET transformation. Beyond elucidating the biochemical pathways of PET transformation, this study provides practical implications for the risk assessment and management of coastal land systems. By identifying key functional taxa (e.g., *Acinetobacter* and *Pseudomonas*), our findings offer a basis for developing microbial indicators to monitor microplastic persistence in the Tiaozini wetland. Such insights are crucial for coastal managers to evaluate the long-term impacts of plastic pollution on soil health and carbon sequestration, ultimately supporting the development of nature-based solutions for the restoration and sustainable use of World Natural Heritage coastal sites.

2. Materials and Methods

2.1. Sample Collection and Microplastic Preparation

Soil samples (0–20 cm depth, approximately 2 kg) were collected from plastic-contaminated areas (32°52′–32°53′ N, 120°56′–120°57′ E) of the Tiaozini World Natural Heritage Site in Dongtai, Jiangsu Province, China. Samples were transported under sterile conditions at 4 °C and used for the enrichment and screening of PET-associated transformation bacteria.

Commercial PET microplastic fibers were used as the primary polymeric substrate in the incubation experiments. The fibers had an average diameter of 16 μm, a length of approximately 6 mm, and a crystallinity of about 30%. The sequential pretreatment with 10% SDS, 75% ethanol, and UV irradiation was used to remove loosely attached dust, residual processing additives, adsorbed organic impurities, and incidental microbial contaminants from the PET fiber surface before incubation. The treated fibers were then vacuum-dried at 60 °C for 48 h before use. The pristine PET fibers were characterized prior to incubation. Scanning electron microscopy (SEM) confirmed a uniform fibrous morphology with smooth and intact surfaces. Fourier transform infrared (FTIR) spectra of the untreated PET exhibited characteristic ester bond absorption peaks, reflecting the initial characteristics of microplastics before incubation. The background microplastic abundance in the source sediment was 1809.18 items kg^{-1}. Polymer identification of representative particles showed that PET accounted for 22.5%, corresponding to an estimated PET abundance of approximately 407.07 items kg^{-1}. These commercially prepared PET fibers served as the defined target substrate for all subsequent incubation, gravimetric analysis, and surface characterization.

2.2. PET-Associated Microbial Enrichment

The liquid and solid media shared the same basal composition; the solid medium was additionally supplemented with agar (10–12 g L^{-1}). PET fibers were used as the primary solid substrate in both media. Two grams of sediment were added into a 50 mL centrifuge tube containing 18 mL of sterile saline. The mixture was shaken for 20 min and then left to stand. The resulting supernatant was used as the microbial inoculum. A total of 5% (v/v) of this sediment suspension was added to 250 mL Erlenmeyer flasks containing the PET medium and incubated at 30 °C, 180 rpm. The control group (CK) was established using the same PET medium composition, PET loading, flask volume, incubation temperature (30 °C), shaking speed (180 rpm), and sampling schedule as the inoculated treatment, except that sterile phosphate-buffered saline was added instead of the microbial suspension. Each group was run in triplicate. Cultures were maintained for 60 days, with regular sampling for microbial and PET-associated transformation analyses.

A mineral salt medium was prepared with PET fibers added as the target substrate. The liquid medium contained Na_2HPO_4 (2.4 g L^{-1}), KH_2PO_4 (1.5 g L^{-1}), $(NH_4)_2SO_4$ (0.5 g L^{-1}), $MgSO_4$ (0.01 g L^{-1}), $CaCl_2$ (0.04 g L^{-1}), and a trace element solution comprising EDTA-2Na (5 mg L^{-1}), $FeSO_4{\cdot}7H_2O$ (2 mg L^{-1}), $ZnSO_4{\cdot}7H_2O$ (0.1 mg L^{-1}), $MnCl_2{\cdot}4H_2O$ (0.03 mg L^{-1}), H_3BO_3 (0.3 mg L^{-1}), $CuCl_2{\cdot}2H_2O$ (0.01 mg L^{-1}), $CoCl_2{\cdot}6H_2O$ (0.2 mg L^{-1}), $NiCl_2{\cdot}6H_2O$ (0.02 mg L^{-1}), and $Na_2MoO_4{\cdot}2H_2O$ (0.03 mg L^{-1}). The pH was adjusted to 7.0 ± 0.2 using sterile 1.0 M HCl. The solid medium had the same basal composition as the liquid medium and was supplemented with agar (10–12 g L^{-1}). PET microplastic fibers (1.00 g per plate) were added as a solid substrate. The pH was adjusted to 7.0 ± 0.2 prior to sterilization.

2.3. Evaluation of PET-Associated Transformation Efficiency and Material Characterization

2.3.1. Weight Loss Measurement

To determine PET-associated transformation, samples were collected every 10 days over a 60-day incubation period. PET fibers were recovered by filtration through a 0.22 µm membrane, rinsed three times with ultrapure water, and vacuum-dried at 60 °C until reaching a constant weight. Fibers were weighed using an analytical balance with 0.1 mg precision. The PET weight loss rate was calculated using the following formula [28]. All recovered fibers used for weight-loss calculation and subsequent physicochemical characterization corresponded to the intentionally added PET substrate.

$$R_{wl} = \frac{w_i - w_f}{w_i} \times 100\% \quad (1)$$

where R_{wl} is the weight loss rate (%), w_i is the initial weight of PET fibers (g), and w_f is the final weight after 60 days (g).

2.3.2. Monitoring of Microbial Biomass and System Turbidity

Microbial growth was monitored by measuring the optical density at 600 nm (OD_{600}). At each sampling time, 1 mL of well-mixed culture broth was collected and, when necessary, diluted with sterile medium to ensure OD_{600} within the linear range of the spectrophotometer. OD_{600} was measured using a UV–vis spectrophotometer (UV-2600, Shimadzu, Kyoto, Japan) at 600 nm, with sterile culture medium used as the blank. The recorded OD_{600} were used as a proxy for overall microbial biomass and system turbidity, rather than a direct quantitative measure of planktonic cell density.

2.3.3. Surface and Chemical Characterization of PET

PET fibers retrieved at days 0, 30, and 60 underwent analysis via SEM, FTIR, and water contact angle (WCA) measurement. For SEM preparation, samples were immersed in 2.5%

glutaraldehyde for 2 h, followed by dehydration in a graded ethanol series (30%, 50%, 70%, 90%, 100%). After critical point drying, samples were gold-coated and observed under a Hitachi SU8600 SEM at 5 kV [29]. For FTIR analysis, PET fibers were mixed with KBr at a 1:100 (*w*/*w*) ratio, pressed into pellets, and scanned across the 4000–400 cm^{-1} range using a Nicolet iS50 spectrometer (Thermo, Waltham, MA, USA), with 32 scans per sample [30]. For WCA assessment, PET fibers were affixed to glass slides, and 5 μL of ultrapure water was deposited onto the surface via a contact angle meter (DSA100, Dataphysics, Filderstadt, Germany) [29]. Five distinct sites per sample were measured, and the average value was recorded.

2.4. Community Structure and Diversity Analysis

2.4.1. Microbial Diversity Sequencing

Microbial genomic DNA was extracted from solid culture media harvested using the CTAB method. DNA concentration and purity were assessed using a NanoDrop spectrophotometer (Thermo, Waltham, MA, USA), and DNA integrity was verified by 1.2% agarose gel electrophoresis. The V3–V4 region of the bacterial 16S rRNA gene was amplified using the universal primers 341F (5′-CCTACGGGNGGCWGCAG-3′) and 805R (5′-GACTACHVGGGTATCTAATCC-3′). PCR products were purified using Vazyme VAHTSTM DNA Clean Beads and quantified with the Quant-iT PicoGreen dsDNA Assay Kit (Thermo, Waltham, MA, USA). Amplicon libraries were prepared using the Illumina TruSeq Nano DNA LT Library Prep Kit (Illumina, San Diego, CA, USA). Sequencing was performed on an Illumina NovaSeq 6000 platform with a paired-end 2 × 250 bp strategy. Raw sequencing reads were processed using QIIME2 (v2019.7). Quality filtering, denoising, and chimera removal were performed using the DADA2 plugin to generate amplicon sequence variants (ASVs). Taxonomic classification was conducted against the Silva (release 132) database. Alpha diversity indices and Beta diversity based on Bray–Curtis dissimilarity (PCoA) were evaluated [31,32]. The raw 16S rRNA gene sequencing data have been deposited in the Genome Sequence Archive (GSA), National Genomics Data Center, Chinese Academy of Sciences, under accession number CRA038523.

2.4.2. Strain Isolation and Identification

After a 60-day enrichment period, the culture broth underwent serial dilution and was spread onto LB agar plates supplemented with PET fibers to recover representative culturable members of the enriched consortium and to enable subsequent strain-level functional assessment. These plates were then incubated at 30 °C for 48 h. Individual colonies were selected and purified via three rounds of repeated streaking. Genomic DNA was isolated from each bacterial isolate, and the full-length 16S rRNA gene was amplified and sequenced. The obtained sequences were compared against entries in the NCBI database to identify the bacterial strains [22].

2.5. Metabolite Analysis of the Culture Medium (GC–MS)

For metabolite extraction from the culture medium, solid-phase extraction (SPE) was employed. SPE columns were initially activated with 5 mL of methanol and 5 mL of ultrapure water. Once the culture solution was filtered through the column, metabolites were eluted using 5 mL of methanol. The eluate was gathered, subjected to rotary evaporation until dry, and then re-dissolved in 100 μL of ethyl acetate. Prior to GC–MS analysis, the solution was filtered through a 0.22 μm membrane.

Gas chromatography–mass spectrometry (GC–MS) analysis was carried out using an Agilent 7890A–5975C system paired with an HP–5MS capillary column (30 m × 0.25 mm × 0.25 μm). The oven temperature was programmed as: maintained at 40 °C for 5 min; ramped to 70 °C at a rate of 2 °C/min and held for 2 min; then increased to 120 °C at 3 °C/min; to 150 °C at 5 °C/min; and finally to 230 °C at 10 °C/min, with a 2-min hold. The flow rate of the

helium carrier gas was set to 1.4 mL/min. The MS scan covered the m/z range of 35–550. Compounds were identified by matching their spectra against records in the NIST 17 mass spectral library [33,34].

2.6. Validation of PET-Associated Transformation by Single Strains and Co-Cultures

2.6.1. Strain Activation and Inoculum Preparation

Four representative bacterial strains were selected from purified single colonies obtained during the late stage of the enrichment process. Each strain was individually inoculated into LB liquid medium and incubated at 30 °C with shaking at 180 rpm for 24 h until reaching the exponential growth phase ($OD_{600} \approx 1.0$). Microorganisms were harvested by centrifugation at 4000 rpm for 10 min, washed three times with sterile saline, and resuspended to an initial optical density of $OD_{600} = 0.1$ to serve as single-strain inoculate.

The four strains selected for subsequent co-culture experiments were based on their high relative abundance in the late stages of enrichment and consistent detection in duplicate samples. These strains represented dominant and functionally related genera in the microbial consortium. The co-culture inoculum was prepared by mixing the four single-strain suspensions at an equal volumetric ratio (1:1:1:1, v/v). This simplified co-culture system was designed to evaluate potential synergistic interactions among core taxa associated with PET-related transformation processes, rather than to reproduce the full taxonomic complexity of the native microbial community.

2.6.2. Experimental Design

PET-associated transformation experiments were conducted in 250 mL Erlenmeyer flasks, each containing 100 mL of PET medium prepared as described in Section 2.2. For the single-strain groups, each flask was inoculated with 5% (v/v) of an individual bacterial suspension, with three biological replicates set up for each strain. In the co-culture group, the same PET medium was inoculated with 5% (v/v) of the mixed-strain suspension, and three replicates were also included. The control group received 5% (v/v) of sterile phosphate-buffered saline (PBS) instead of the microbial inoculum. All flasks were incubated at 30 °C with shaking at 180 rpm for 60 days.

2.7. Statistical Analysis of Data

In this work, experimental data were organized using Microsoft Excel 2021. Statistical analyses were conducted with SPSS 27.0 (IBM Corp., Armonk, NY, USA). Graphical visualizations were generated using Origin 2022 (OriginLab, Northampton, MA, USA). Microbial diversity metrics were calculated using the 'vegan' and 'ggplot2' packages in R (version 4.4.1). Phylogenetic analyses were performed with MEGA 12.0. Differences in PET weight loss among treatments were assessed using one-way analysis of variance (ANOVA), with $p < 0.05$ considered statistically significant. Differences in microbial consortium composition were evaluated using permutational multivariate analysis of variance (PERMANOVA) based on Bray–Curtis distances.

3. Results

3.1. Microbial Community Responses During PET-Associated Incubation

3.1.1. Community Microbial Growth

The temporal variation of OD_{600} of microbial communities during incubation in the PET-containing system is shown in Figure 1. In the inoculated group, OD_{600} values increased from day 0 to day 50, reaching a maximum of 1.65 ± 0.04, followed by a slight decrease at day 60. These changes likely reflect system-level alterations in microbial biomass, aggregation, and physiological status during prolonged incubation. In contrast,

the control group (CK), which lacked microbial inoculation, maintained consistently low OD_{600} (<0.1) throughout the incubation period. In summary, these observations indicate pronounced microbial responses at the community-level under PET-containing conditions.

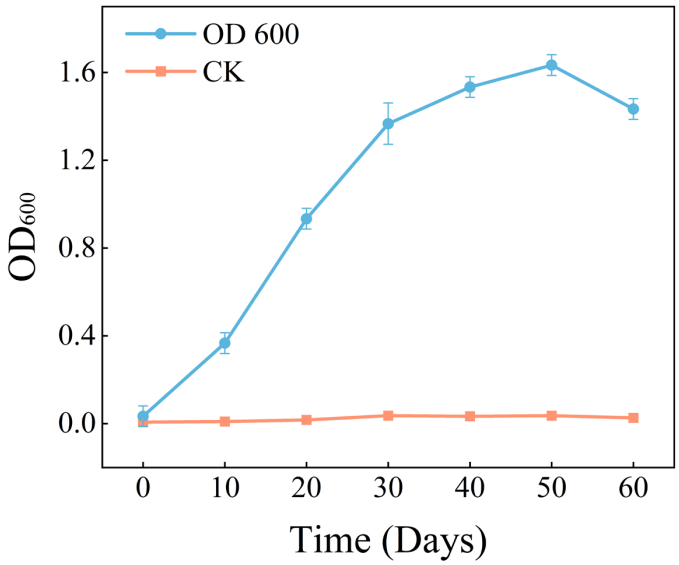


Figure 1. Temporal changes in OD_{600} of the inoculated microbial consortium and the control (CK) during 60 days of incubation in PET-containing medium.

3.1.2. PET-Associated Transformation Performance at the Community-Level

The temporal changes in PET weight loss in the inoculated and CK groups are shown in Figure 2. In the inoculated group, PET weight loss increased progressively over the 60-day incubation period, reaching 13.7 ± 0.9% by day 60, indicating sustained PET-associated mass loss over time. In contrast, the abiotic control group exhibited minimal changes in PET mass (<2%) throughout the experiment. The minor mass loss observed in CK groups may be attributed to abiotic processes, such as the leaching of additives, processing aids, and other extractable components. Similar abiotic mass loss has also been reported in previous studies and is considered an inherent phenomenon in liquid-based experimental systems [32,33]. The difference in PET mass loss between the inoculated and control groups further indicates a pronounced interaction between microorganisms and PET.

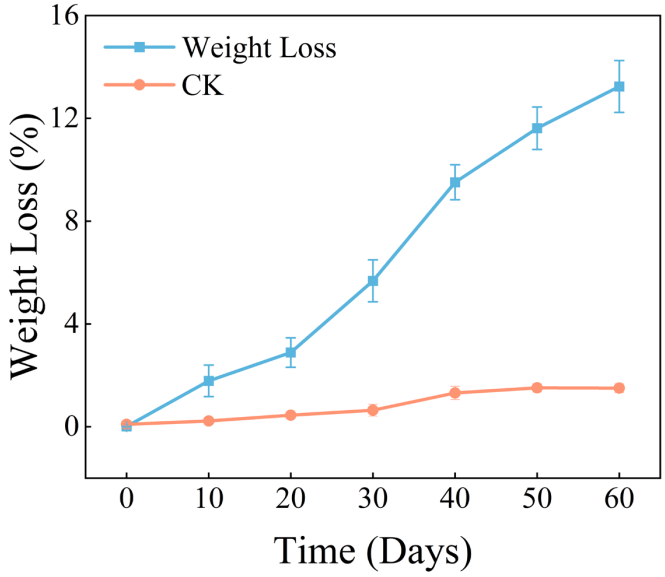


Figure 2. Temporal changes in PET mass loss in the inoculated and control groups.

3.2. PET-Associated Physicochemical Changes Under Incubation Conditions

3.2.1. Surface Morphology and Hydrophilicity of PET Fibers

SEM images of PET fibers after 0, 30, and 60 days of microbial incubation are shown in Figure 3a–c. At day 0, the PET surface appeared smooth and intact, with no visible signs of erosion. After 30 days of incubation, the PET surface became rougher, and microbial colonization became evident. However, the microorganisms remained relatively sparsely distributed. By day 60 of incubation, pronounced microbial enrichment and well-defined microbial colonies were observed on the PET surface, accompanied by discernible erosion features. These observations suggest a potential interaction between microorganisms and PET, which may further account for the trends observed in OD_{600} and PET mass loss.

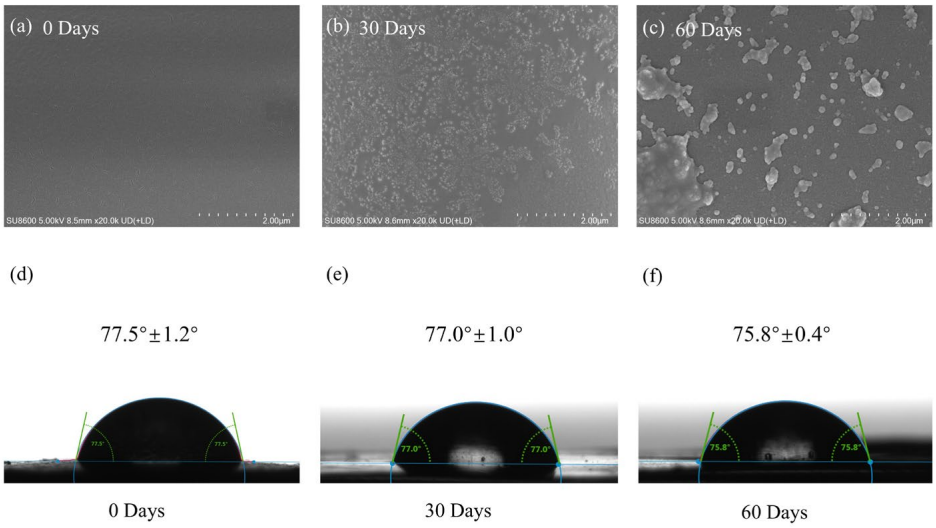


Figure 3. Changes in PET surface morphology (**a**–**c**) and water contact angle (**d**–**f**) during 60 days of incubation. (**a**–**c**) SEM images of PET surfaces at 0, 30, and 60 days, respectively. (**d**–**f**) Corresponding water contact angles showing a gradual decrease from 77.5 ± 1.2° (day 0), 77.0 ± 1.0° (day 30), to 75.8 ± 0.4° (day 60), indicating increased surface hydrophilicity.

The WCA values of PET at different incubation times are shown in Figure 3d–f, reflecting changes in the surface hydrophilicity of the microplastics. The initial WCA of the PET surface was 77.5 ± 1.2°, indicating moderate surface hydrophilicity of the pristine PET. After 30 days of incubation, the WCA showed a decreasing trend, declining to 77.0 ± 1.0°, suggesting an influence of initial microbial enrichment on the surface properties of PET. By day 60 of incubation, the WCA exhibited a more pronounced decrease compared with that at 30 days, reaching 75.8 ± 0.4°. Combined with the pronounced microbial enrichment observed on the PET surface, the decrease in WCA from 77.5 ± 1.2° at day 0 to 75.8 ± 0.4° at day 60 suggests that microbial colonization was associated with enhanced PET surface hydrophilicity during incubation. The changes in PET surface hydrophilicity reflect not only microbial enrichment but also microbially induced alterations in surface properties, such as functional groups, highlighting the interaction between PET and microorganisms. The original WCA measurements are provided in Table S1 of the Supplementary Materials.

3.2.2. Chemical Structure Changes in PET Revealed by FTIR Analysis

The FTIR spectra of PET microplastics before and after microbial incubation are shown in Figure 4. Notably, compared with pristine PET (ORI, untreated PET), microbially treated PET (TRE) exhibited a pronounced broad absorption band at approximately 3315.0 cm^{-1}, which is assigned to O-H stretching vibrations. These results suggest that microbial enrichment on the PET surface led to an increase in hydrophilic functional groups, such as -OH,

on the microplastics. This observation helps explain the microbially induced enhancement of PET hydrophilicity and provides evidence for microbial involvement in PET-associated transformation. In addition to the -OH groups, compared with pristine PET, microbially treated PET exhibited slight blue and red shifts near 1710.1 cm^{-1} and 1241.6 cm^{-1}, corresponding to the C=O and C-O-C functional groups, respectively. These spectral shifts indicate that microbial enrichment altered the chemical environment of hydrophilic functional groups on the PET surface, further contributing to changes in surface hydrophilicity. Moreover, variations in several absorption bands at 1610.4 cm^{-1}, 1092.0 cm^{-1}, 1018.0 cm^{-1}, and 872.8 cm^{-1} collectively suggest microbially induced modifications to the surface properties of PET.

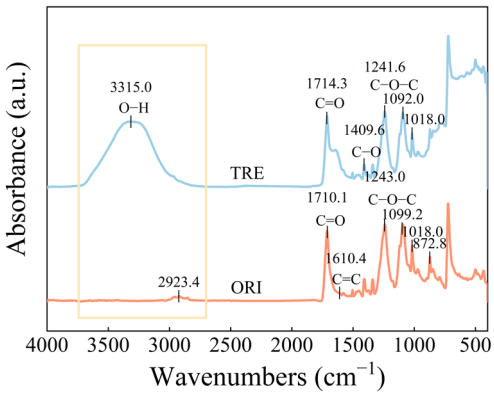


Figure 4. FTIR spectra of TRE (blue curve) and ORI (red curve). The yellow border highlights the region with obvious spectral changes. Peaks corresponding to characteristic functional groups (O-H, C=O, C=C, C-O, C-O-C) are labeled with their wavenumbers (cm^{-1}). TRE refers to PET samples after microbial treatment, whereas ORI denotes pristine untreated PET fibers.

3.3. Temporal Dynamics of Microbial Community Composition and Diversity

3.3.1. Changes in α-Diversity

During incubation under PET-present conditions, both microbial community diversity (Shannon index) and richness (Chao1 index) displayed clear temporal variations, as illustrated in Figure 5a. During the first 20 days, the Shannon index increased markedly, indicating a rapid diversification of the community during early colonization. Thereafter, Shannon values stabilized and slightly declined toward the end of incubation, suggesting increasing selection for PET-adapted taxa. In contrast, the Chao1 index showed an overall increasing trend throughout the 60-day period, indicating continued accumulation of taxonomic richness. Taken together, these patterns suggest that PET exposure promoted initial diversification followed by progressive ecological filtering, leading to higher richness but a more selectively structured community at later stages.

3.3.2. Changes in β-Diversity

The successional dynamics of the microbial consortium were examined using representative samples collected from each enrichment phase to characterize changes in taxonomic richness and community structure. As shown in Figure 5b, the number of ASVs. across taxonomic ranks from phylum to species increased progressively throughout the incubation period. Notably, the number of ASVs exhibited clear associations with the temporal patterns of both the Shannon and Chao1 indices. During the first three stages, concurrent increases in microbial diversity and richness were observed, which were consistent with the increase in ASV numbers. In the fourth stage, a synchronous decline in all three metrics further supports their close association. Interestingly, in the fifth stage, the Shannon index did not show a pronounced increase, whereas both the Chao1 index and ASV numbers

continued to rise. This pattern is not contradictory but instead reflects the selective role of PET as a substrate in shaping the microbial community. When environmental conditions were not strongly influenced by PET, the overall activity of PET-associated microorganisms appeared relatively low, which may be related to the protected status of the study area. In contrast, when PET became a dominant substrate, PET-associated microorganisms exhibited increases not only in abundance but also in diversity. Overall, the selective effect of PET was manifested by the enrichment and diversification of PET-utilizing microorganisms, while microbial taxa not associated with PET utilization may have been suppressed.

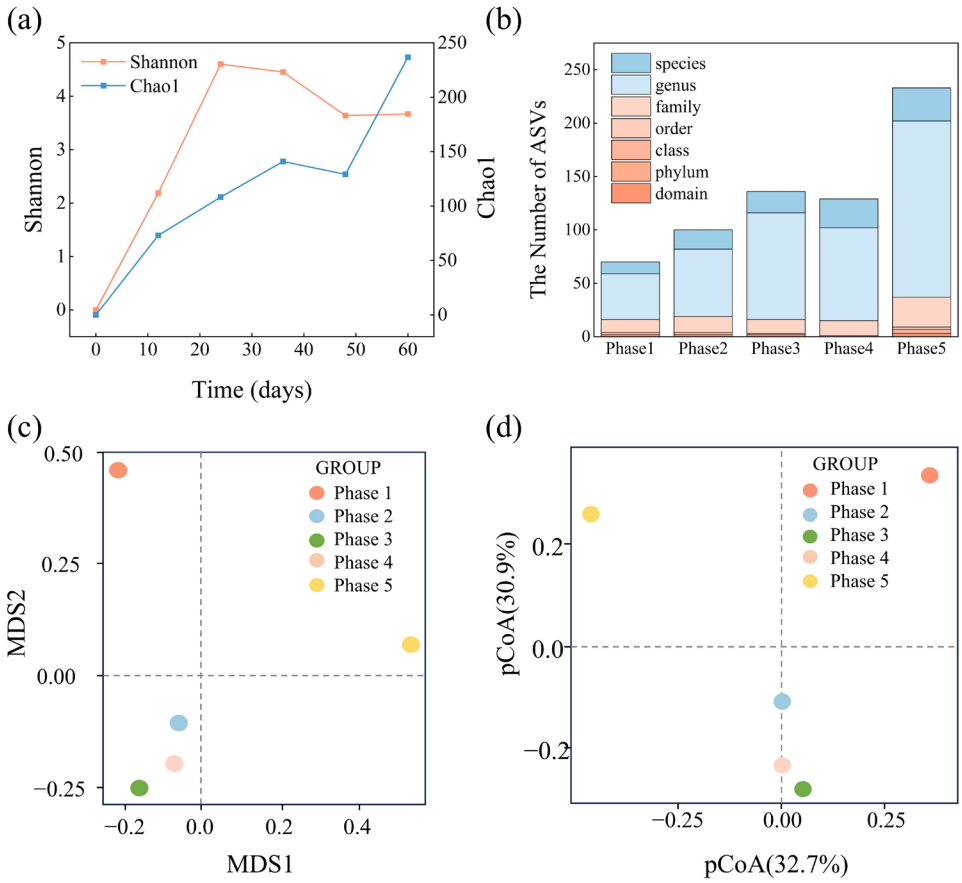


Figure 5. Microbial consortium diversity: (**a**) microbial αdiversity (Shannon index and Chao1 index); (**b**) distribution of the number of ASVs at different taxonomic levels; (**c**) community structure cluster analysis based on MDS; (**d**) community structure cluster analysis based on PCoA. The dashed lines in panels (**c**,**d**) indicate the zero values of the ordination axes.

Temporal shifts in community composition were further resolved using multidimensional scaling (MDS) and PCoA based on Bray–Curtis dissimilarity (Figure 5c,d). Both ordination approaches revealed a clear temporal separation of samples along the incubation timeline, consistent with a directional successional trajectory. PERMANOVA analysis confirmed that β-diversity differences among enrichment phases were statistically significant ($p < 0.05$), and pairwise comparisons indicated significant compositional differences between successive phases (all $p < 0.05$). Together, these results demonstrate that PET microplastics exerted sustained selective pressure, driving continuous and stage-specific restructuring of the indigenous wetland microbial community over time.

3.3.3. Succession of Dominant Genera and Species of Microbial Communities

Temporal changes in the relative abundance of dominant bacterial genera across the five incubation phases (Phase 1–Phase 5) revealed a clear successional pattern (Figure 6a).

During the early incubation stages (Phase 1–Phase 3), *Acinetobacter* dominated the microbial consortium, accounting for more than 60% of the total community. This early dominance coincided with increased microbial biomass and the onset of measurable PET-associated mass loss, indicating active microbe-plastic interactions under PET-containing conditions.

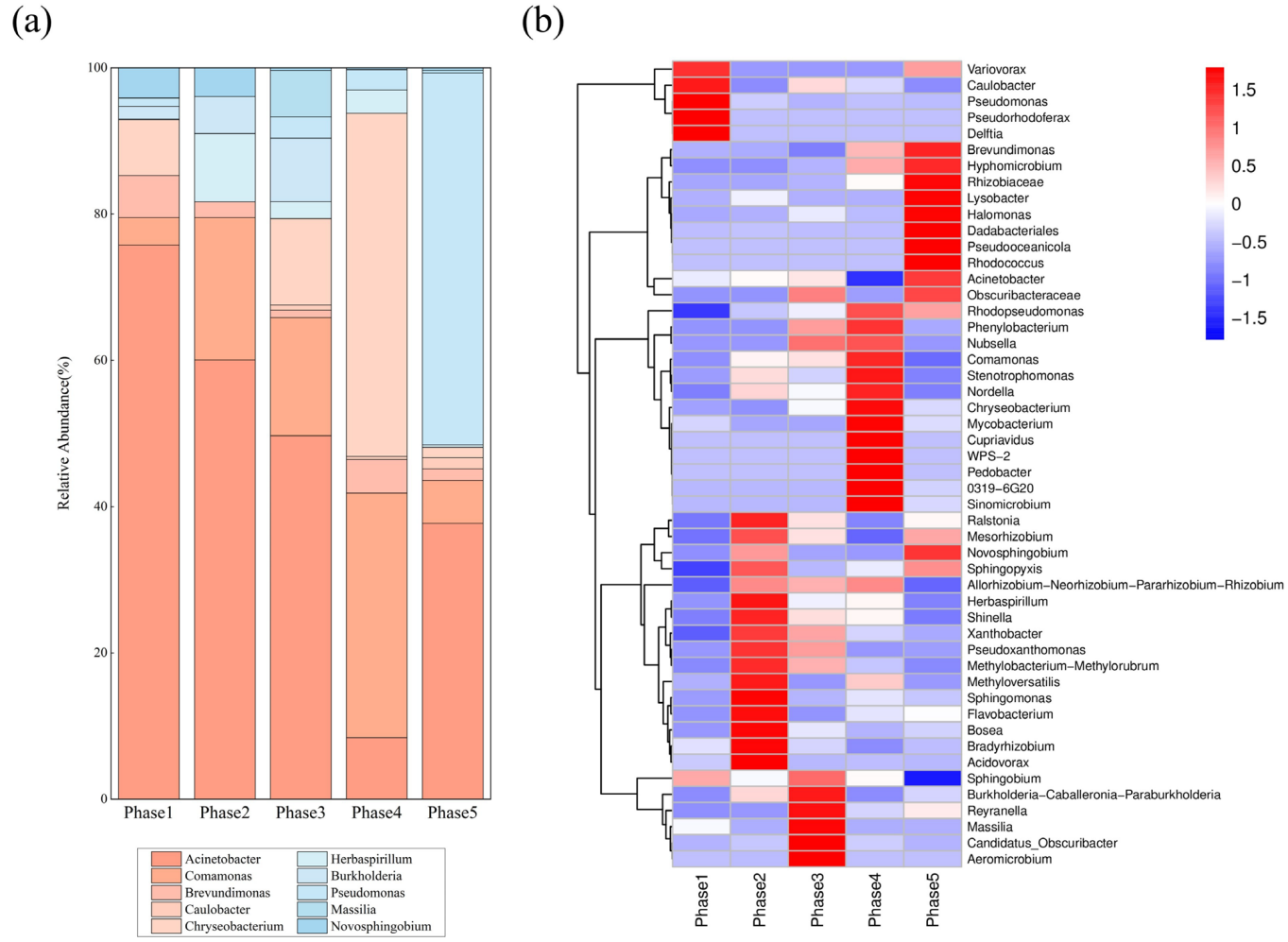


Figure 6. Phase-dependent microbial succession and community restructuring during PET-associated transformation at both genus and species levels. (**a**) shows the relative abundance of dominant genera during PET-associated transformation across Phase 1 to Phase 5; (**b**) shows the species-phase correlation heat map.

From Phase 4 to Phase 5, the relative abundance of *Acinetobacter* gradually declined, while *Pseudomonas* and *Massilia* showed marked enrichment. By Phase 5, *Pseudomonas* became the dominant genus, exceeding 40% relative abundance. This taxonomic shift occurred alongside progressive PET surface modifications, including enhanced microbial colonization, decreased water contact angle, and increased surface hydrophilicity. Together, these results indicate that PET microplastics imposed sustained selective pressure on the microbial community, driving a transition from early surface colonizers to taxa potentially involved in downstream PET-associated transformation processes and providing a basis for subsequent strain isolation and functional verification.

3.3.4. Characterization of the Abundance Distribution of Functional Pathways in Microbial Communities

The predicted functional profile based on KEGG annotation (Figure 7) was dominated by metabolism-related pathways, with amino acid, carbohydrate, and lipid metabolism

being particularly abundant. Pathways involved in genetic information processing, including replication, repair, and translation, were also well represented. This functional pattern indicates that the microbial consortium maintained strong metabolic capacity and active cellular processes during incubation under PET-containing conditions, supporting sustained community growth and succession. As these results are derived from 16S rRNA gene-based predictions, they reflect the potential functional capacity of the consortium rather than direct evidence of specific metabolic activities. Nevertheless, the predominance of central metabolic and cellular maintenance functions is consistent with the observed microbial proliferation, surface colonization, and PET-associated physicochemical transformation observed in this study. These pathway annotations should therefore be interpreted as ecological potential rather than direct evidence of enzyme expression or in situ metabolic flux.

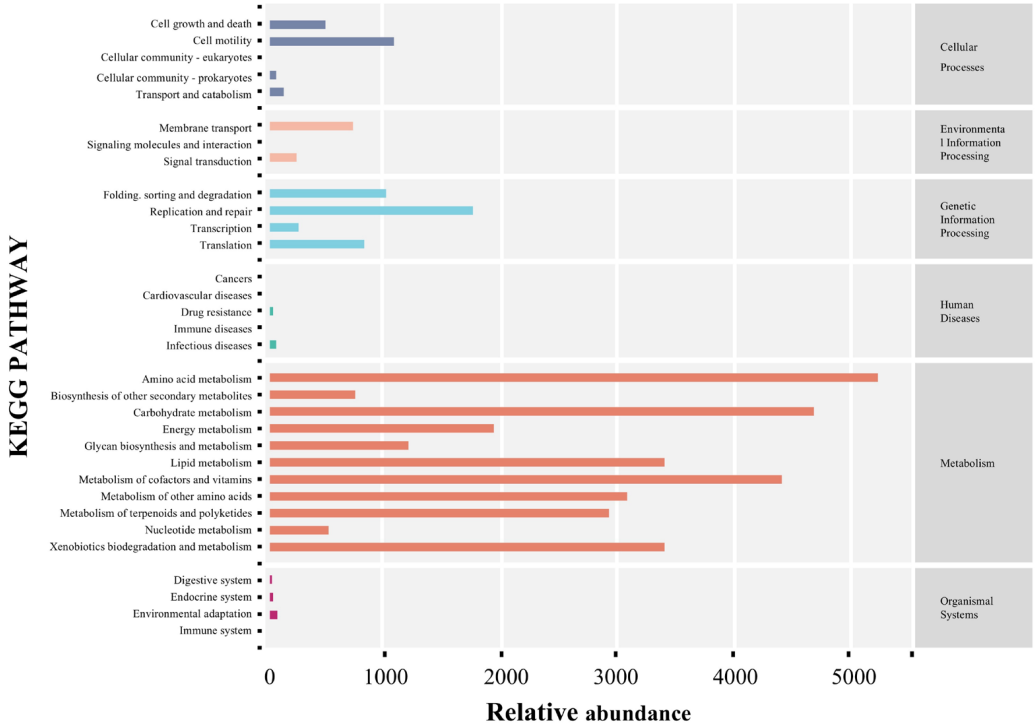


Figure 7. KEGG pathway annotation and classification. Different colors represent different KEGG level-1 categories, including Cellular Processes, Environmental Information Processing, Genetic Information Processing, Human Diseases, Metabolism, and Organismal Systems.

3.4. GC–MS Analysis of Metabolites Detected During Microbial Incubation with PET

To further assess chemical changes occurring within the culture system during microbial incubation with PET, extracellular metabolites in the culture medium were analyzed by GC–MS (Figure 8). Comparison of total ion chromatograms (TICs) revealed clear differences between ORI and TRE, including the appearance of a distinct peak at approximately 23.2 min in the treated sample that was absent in the control. Quantitative analysis of selected compounds showed pronounced shifts in relative peak area distributions, with Compound A exhibiting a substantial increase in the treated system, while other detected compounds remained at comparable levels between treatments. These results indicate that prolonged microbial incubation in the presence of PET was accompanied by measurable changes in the chemical composition of the surrounding medium.

The altered GC–MS profiles are more plausibly interpreted as reflecting microbial metabolic activity, including co-metabolic by product formation and secondary chemical transformations occurring during community growth and PET surface association. When considered together with PET mass loss, SEM-observed surface erosion, increased surface

hydrophilicity, and FTIR-detected functional group modifications, the GC–MS results provide complementary evidence for PET-associated, microbially mediated physicochemical modification at the system level.

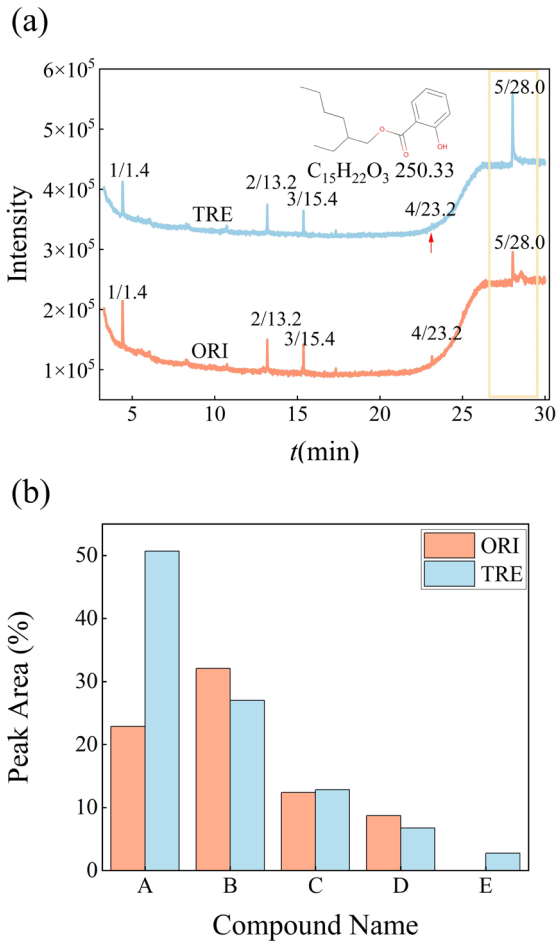


Figure 8. GC–MS analysis of metabolites detected during PET-associated transformation. (**a**) GC-MS TIC; (**b**) comparison of peak areas of the characteristic products: A: 13-Docosenamide, (Z)-; B: Cyclohexasiloxane, dodecamethyl; C: 5-Amino-1-benzene-6-hydroxypyrimidine; D: 2,4 (1H,3H)-dione, 4-TMS; E: 2-Ethylhexyl salicylate. The red arrow indicates the characteristic differential signal near 23.2 min in TRE, and the yellow box highlights the late-retention-time region with pronounced differences between TRE and ORI.

3.5. Screening and Verification of Functional Strains from PET Enrichment Cultures

3.5.1. Isolation and Identification of Strains

To characterize the cultivable microbial members present during the enrichment process, four dominant bacterial strains were isolated from the incubation system. Their 16S rRNA genes were sequenced and subjected to phylogenetic analysis, and the resulting neighbor-joining trees are shown in Figure 9. In the phylogenetic tree of the genus *Stenotrophomonas* (Figure 9a), the isolated strain clustered closely with *Stenotrophomonas chelatiphaga* and *Stenotrophomonas* geniculata, forming a well-supported branch (bootstrap $\geq$ 78). Figure 9b shows the phylogenetic placement of the isolated strain within the genus *Streptomyces*, where it was closely related to *Streptomyces mutabilis* and *Streptomyces rochei*. The isolate shown in Figure 9c was classified within the genus *Massilia* and exhibited close phylogenetic affinity to *Pseudoduganella lurida*. The isolate presented in Figure 9d belonged to the genus *Pseudomonas* and clustered with *Pseudomonas fildesensis* and *Pseudomonas cedrina*. These phylogenetic affiliations indicate that the enrichment strategy enabled the recovery of cultivable bacterial taxa commonly associated with plastic-containing and sedimentary environments. The

isolation of these strains provides a practical link between the observed community-level PET-associated responses and subsequent strain-level functional assessments. This connection allows the enriched consortium to be further examined using simplified culture systems, facilitating targeted evaluation of PET-associated transformation processes.

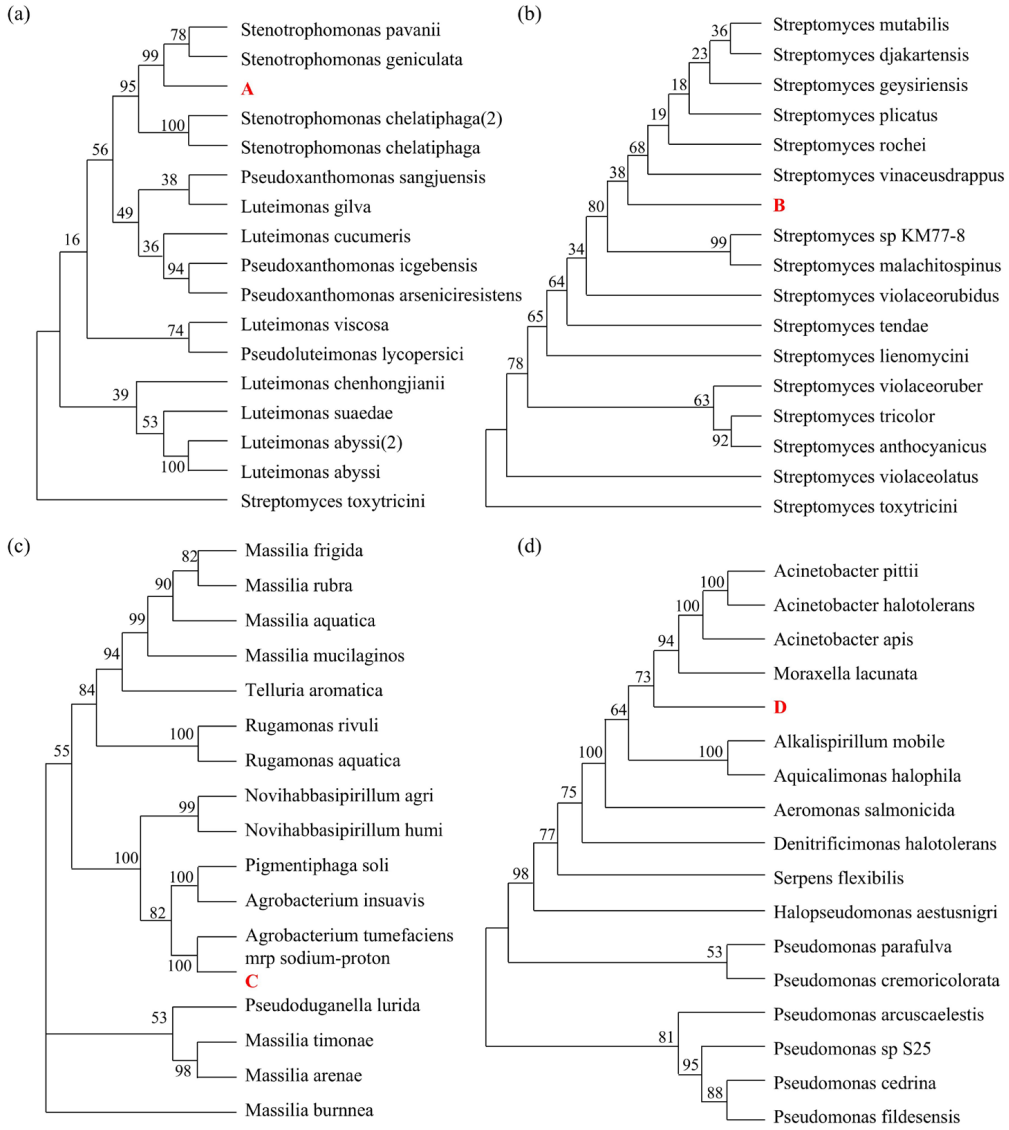


Figure 9. Phylogenetic identification of cultivable PET-associated microorganisms. Panels (**a**–**d**) show neighbor-joining phylogenetic trees of representative isolates affiliated with *Stenotrophomonas*, *Streptomyces*, *Massilia*, and *Pseudomonas*, respectively. The red letters A–D indicate the four representative isolates selected for subsequent validation assays.

3.5.2. Functional Comparison of Isolated Strains in PET-Associated Transformation

As shown in Figure 10, representative strains isolated from the consortium were evaluated under monoculture and co-culture conditions to verify their PET-associated transformation potential. After 60 days of incubation, PET weight loss differed significantly among treatments (one-way ANOVA, $p < 0.05$). Among the individual strains, *Stenotrophomonas maltophilia* exhibited the highest PET-associated weight loss (3.2 ± 0.1%), followed by *Pseudomonas* sp. (2.3 ± 0.1%), *Streptomyces* sp. (2.1 ± 0.1%), and *Massilia* sp. (1.7 ± 0.1%).

When the four strains were co-cultured at an equal volume ratio (1:1:1:1), PET weight loss reached 9.2 ± 0.1%, which was significantly higher than that observed for any individ-

ual strain ($p < 0.05$), but remained lower than the PET-associated mass loss measured for the original enriched microbial consortium (13.2 ± 1.1%). The strain-level assays provide functional support for the community-level patterns observed during enrichment. While individual isolates induced only limited PET-associated mass loss, their co-culture produced a clearly enhanced transformation effect, indicating the importance of interspecies interactions. The four-strain system did not fully reproduce the transformation capacity of the original enriched consortium. This suggests that additional low-abundance or uncultivated taxa, as well as more complex metabolic interactions, contribute to PET-associated processes. Taken together, these results, in combination with the observed community succession, indicate that PET-associated transformation in wetland sediments is more likely driven by functionally complementary microbial assemblages than by any single dominant taxon.

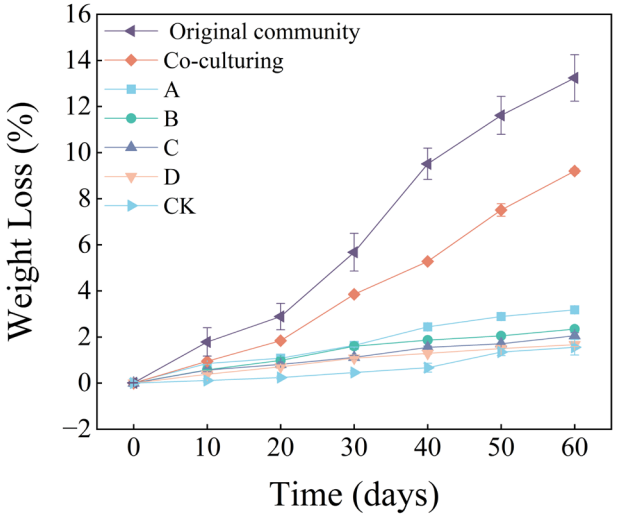


Figure 10. PET weight loss percentages over a 60-day incubation period under different microbial treatments. Original community represents the PET-associated transformation performance of the enriched native microbial consortium. Co-culturing denotes the combined treatment of the four isolated strains mixed at an equal volume ratio (1:1:1:1). A, B, C, and D represent monocultures of the individual isolates (*Stenotrophomonas maltophilia*, *Pseudomonas* sp., *Streptomyces* sp., and *Massilia* sp., respectively). CK indicates the sterile control without microbial inoculation. Error bars represent standard deviations ($n = 3$).

4. Discussion

4.1. PET-Associated Transformation Under Environmentally Relevant Conditions

In this study, the wetland-derived microbial consortium achieved a 13.2% mass loss of PET microplastics over 60 days. This level of mass loss falls within the range reported for environmentally derived microbial consortia [35–38]. In environmental or nature-derived systems, indigenous microbial communities and consortia have been shown to induce measurable PET microplastic transformation over comparable time scales. For example, a two-stage natural microbial consortium strategy reported approximately 28 ± 2% PET mass loss over 60 days, highlighting the role of community-level interactions and sequential processing in complex microbial systems [39].

This disparity suggests that PET-associated transformation in coastal sediments is primarily mediated at the community-level. Compared with single isolates, microbial consortia may facilitate sequential and complementary metabolic processes. Although Li et al. [40] investigated polyethylene rather than PET, their results similarly indicated that community-level interactions could enhance plastic biodegradation beyond the capacity of individual members, lending support to our interpretation that metabolic complementarity

among taxa contributed to the higher PET-associated mass loss observed in the native wetland consortium.

Consistent with previous observations, SEM and FTIR analyses confirmed that PET microplastics underwent progressive surface erosion and chemical restructuring [37,41,42]. Importantly, these changes reflect PET-associated transformation rather than exhaustive mineralization [43]. In wetland environments, microplastics tend to function as persistent solid scaffolds, providing long lived surfaces for microbial colonization and ecological interaction [44,45]. Accordingly, the observed mass loss is more plausibly attributed to selective microbial utilization of accessible functional groups in combination with the leaching of low molecular weight fragment [46]. Together, these findings indicate that wetland-derived microbial communities are capable of mediating PET-associated transformation at environmentally relevant temperatures, with outcomes shaped by both community interactions and polymer substrate characteristics [21,26,27].

4.2. PET Microplastics as Selective Scaffolds Shaping Microbial Community Structure

Beyond measurable mass loss, PET microplastics exerted a pronounced influence on microbial community structure throughout the incubation period. β-diversity analyses and ordination results revealed a clear and reproducible successional trajectory, indicating that PET acted as a persistent selective pressure rather than a passive background material. This pattern is consistent with the plastisphere concept, which frames microplastics as long-lived ecological niches that support microbial assemblages distinct from surrounding sediments [47,48].

In the present system, PET fibers represented the dominant external solid substrate introduced into the sediment-derived enrichment culture. Under these conditions, microbial taxa capable of surface colonization, biofilm formation, or interaction with polymer-associated transformation products were selectively favored [40,49]. The progressive separation of community composition across incubation phases, supported by PERMANOVA results, suggests that the observed succession was not driven by stochastic drift, but instead reflected substrate-driven selection imposed by the PET microplastics [43].

4.3. Deterministic Succession and Division of Labor Within the Microbial Consortium

In response to this selective enrichment, a clear taxonomic succession was observed, characterized by an early dominance of *Acinetobacter* followed by increased prevalence of *Pseudomonas*, *Massilia*, and *Streptomyces* in later incubation stages. This successional pattern provides a functional roadmap for PET-associated transformation and aligns with plastisphere-associated succession reported across diverse ecosystems, where early surface colonizers are gradually supplemented or replaced by taxa specialized in downstream metabolic processes [48,50–52]. The early enrichment of *Acinetobacter* is likely attributable to its strong surface-attachment and biofilm-forming capabilities on hydrophobic substrates [53], facilitated by biosurfactant production and extracellular polymeric substance secretion [54]. Such biophysical priming enhances surface wettability and stabilizes microbial attachment, effectively conditioning the PET surface for subsequent colonization [21]. As incubation progressed, the increased abundance of *Pseudomonas* suggests a functional shift toward taxa with broader metabolic versatility, including esterase- and hydrolase-associated pathways capable of processing ester bonds or PET-derived low molecular-weight intermediates [55,56]. Concurrent enrichment of *Streptomyces* further implies the establishment of metabolic niches related to the processing of aromatic compounds, such as terephthalate derived products [57].

Collectively, these observations support a division-of-labor framework, in which early colonizers modify the physical and chemical properties of the substrate, thereby

enabling later arriving specialists to perform downstream biochemical transformations. This cooperative succession offers a mechanistic explanation for the enhanced PET-transforming capacity of microbial consortia relative to individual strains and reinforces the view that PET-associated transformation in coastal sediments is a deterministic, community-driven process.

4.4. Functional Constraints Inferred from Strain-Level Assays and Chemical Signatures

Strain-level assays impose clear constraints on the interpretation of PET-associated transformation observed at the community-level. While co-cultivation of representative isolates enhanced PET-associated mass loss compared with monocultures, the simplified system did not reproduce the transformation capacity of the native consortium. This gap indicates that PET-associated processes in wetland sediments likely rely on broader community interactions, including contributions from low-abundance, uncultivated, or syntrophic taxa that are not retained during isolation.

Chemical evidence further constrains mechanistic interpretation. Although GC–MS revealed altered extracellular metabolite profiles during incubation, canonical PET depolymerization intermediates were not detected. This absence may reflect rapid microbial uptake, concentrations below detection limits, or analytical constraints associated with non-derivatized GC–MS analysis of polar compounds [58]. Combined with SEM- and FTIR-based evidence of surface erosion and functional group modification, these findings suggest that microbial activity primarily drives surface-associated physicochemical modification and co-metabolic transformation. Together, the strain-level and chemical data indicate that early PET transformation in wetland sediments is limited by community complexity and timescale, with complete mineralization likely requiring prolonged incubation and more integrated microbial partnerships.

4.5. Implications for Coastal Wetland Land Systems

The results of this study have important implications for the management and conservation of coastal wetland land systems subjected to long-term microplastic accumulation. The observed PET-associated transformation mediated by indigenous microbial communities indicates that coastal wetlands possess an inherent capacity for the natural attenuation of microplastics through community-level physicochemical and biological processes. Rather than relying exclusively on rapid removal or engineered remediation, such intrinsic microbial functions may contribute to the gradual reduction in microplastic-associated risks in sedimentary environments.

In protected wetlands such as the Tiaozini Wetland, a World Natural Heritage Site, maintaining the integrity of sediment microbial habitats is critical. Indigenous microbial communities adapted to persistent plastic substrates and complex redox conditions play a stabilizing role in sediment biogeochemical functioning. Excessive anthropogenic disturbance, including large scale dredging, sediment replacement, or intensive physicochemical treatment, can disrupt microbial networks and weaken the wetland's self-purification capacity. From a land management perspective, conservation-oriented strategies that prioritize habitat preservation, maintenance of natural hydrological regimes, and minimal intervention are more likely to sustain microbial processes underlying natural attenuation. Although microbial transformation alone cannot fully eliminate microplastics, it represents a complementary and ecologically sustainable component of long-term wetland management and restoration frameworks [59,60].

4.6. Limitations and Future Perspectives

A limitation of the present study is that PET-associated transformation was inferred primarily from mass loss, surface modification, and extracellular metabolite profiles, whereas specific enzymatic activities and functional genes were not directly quantified. In addi-

tion, the enrichment cultures were established under controlled laboratory conditions, which inevitably simplified the spatial heterogeneity and physicochemical dynamics of natural coastal wetlands. The reduced performance of the synthetic co-culture relative to the native consortium further suggests that uncultivated or low-abundance taxa may contribute to cross-feeding and intermediate turnover. Although background microplastics were present in the source sediment (1809.18 items kg^{-1}), polymer identification of representative particles indicated that PET accounted for 22.5%, corresponding to an estimated PET abundance of approximately 407.07 items kg^{-1}. Relative to the intentionally added commercial PET fibers used in the incubation system, the abundance of indigenous PET particles was low and therefore unlikely to have dominated the observed gravimetric loss and surface-associated changes in the added PET substrate. However, these indigenous particles may have contributed to the prior environmental exposure history and initial selective background of the microbial community. Future studies integrating community-resolved omics approaches with longer-term or field-based incubations will help refine the mechanistic understanding and ecological relevance of microbial PET transformation in wetland systems.

5. Conclusions

This study shows that wetland-derived microbial communities can mediate PET microplastic transformation under environmentally relevant conditions. Long-term incubation resulted in measurable PET mass loss, surface erosion, increased hydrophilicity, and functional group modifications, indicating sustained microbe–plastic interactions rather than rapid polymer mineralization. Community analyses revealed clear microbial succession in the presence of PET, while strain-level assays confirmed that cooperative interactions enhanced PET-associated transformation. Although simplified co-cultures did not fully reproduce the activity of the native consortium, they demonstrated that PET transformation is a community-driven process. Together, these results verify the presence of PET-transforming microorganisms in coastal wetland sediments and clarify key features of the transformation process, including surface conditioning and co-metabolic interactions. The findings highlight the ecological role of sediment microbial communities in the long-term attenuation of microplastics in wetland land systems. Future work should combine metagenomics, transcriptomics, enzyme assays, and longer-term field-relevant incubations to verify the functional mechanisms and ecological significance of PET transformation in coastal wetlands.

Supplementary Materials: The following supporting information can be downloaded at: https://www.mdpi.com/article/10.3390/land15030495/s1. Table S1. Original WCA measurements of PET fibers at different incubation times.

Author Contributions: Conceptualization, W.Z.; Funding acquisition, D.Z.; Investigation, J.D.; Methodology, Z.Z.; Validation, J.R.; Writing—original draft, J.D.; Writing—review & editing, G.L., Z.L. and S.X. All authors have read and agreed to the published version of the manuscript.

Funding: This research was funded by the Young Elite Scientists Sponsorship Program by the China Association for Science and Technology (CAST) under Grant No. 2023QNRC001, the Tianfu Emei Talent Program (No. 1943), and the Dongtai-Fudan Joint Innovation Center for Wetland Protection.

Data Availability Statement: The raw sequence data generated in this study have been deposited in the Genome Sequence Archive (GSA), National Genomics Data Center (NGDC), China National Center for Bioinformation, Chinese Academy of Sciences, under accession number CRA038523. The data are publicly accessible at https://ngdc.cncb.ac.cn/gsa (accessed on 9 February 2026). Additional data supporting the findings of this study are available from the corresponding authors upon reasonable request.

Acknowledgments: We are thankful for the Young Elite Scientists Sponsorship Program, Tianfu Emei Talent Program and the Dongtai-Fudan Joint Innovation Center for Wetland Protection.

Conflicts of Interest: Author Dan Zhou was employed by the company Yancheng Tiaozini Wetland Research Institute Co., Ltd. The remaining authors declare that the research was conducted in the absence of any commercial or financial relationships that could be construed as a potential conflict of interest.

References

1. Vázquez, O.A.; Rahman, M.S. An Ecotoxicological Approach to Microplastics on Terrestrial and Aquatic Organisms: A Systematic Review in Assessment, Monitoring and Biological Impact. *Environ. Toxicol. Pharmacol.* **2021**, *84*, 103615. [CrossRef]
2. Thompson, R.C.; Swan, S.H.; Moore, C.J.; vom Saal, F.S. Our Plastic Age. *Philos. Trans. R. Soc. B Biol. Sci.* **2009**, *364*, 1973–1976. [CrossRef]
3. Wright, S.L.; Thompson, R.C.; Galloway, T.S. The Physical Impacts of Microplastics on Marine Organisms: A Review. *Environ. Pollut.* **2013**, *178*, 483–492. [CrossRef] [PubMed]
4. Geyer, R.; Jambeck, J.R.; Law, K.L. Production, Use, and Fate of All Plastics Ever Made. *Sci. Adv.* **2017**, *3*, e1700782. [CrossRef] [PubMed]
5. Nisticò, R. Polyethylene Terephthalate (PET) in the Packaging Industry. *Polym. Test.* **2020**, *90*, 106707. [CrossRef]
6. Huang, J.-N.; Wen, B.; Zhu, J.-G.; Zhang, Y.-S.; Gao, J.-Z.; Chen, Z.-Z. Exposure to Microplastics Impairs Digestive Performance, Stimulates Immune Response and Induces Microbiota Dysbiosis in the Gut of Juvenile Guppy (*Poecilia reticulata*). *Sci. Total Environ.* **2020**, *733*, 138929. [CrossRef]
7. Li, N.; Wu, M.; Zhang, Y.; Yuan, W.; Wu, J.; Shao, X. A Review on Microplastics Pollution in Coastal Wetlands. *Watershed Ecol. Environ.* **2023**, *5*, 24–37. [CrossRef]
8. Eerkes-Medrano, D.; Thompson, R.C.; Aldridge, D.C. Microplastics in Freshwater Systems: A Review of the Emerging Threats, Identification of Knowledge Gaps and Prioritisation of Research Needs. *Water Res.* **2015**, *75*, 63–82. [CrossRef]
9. Liu, Y.; Zhang, J.; Cai, C.; He, Y.; Chen, L.; Xiong, X.; Huang, H.; Tao, S.; Liu, W. Occurrence and Characteristics of Microplastics in the Haihe River: An Investigation of a Seagoing River Flowing through a Megacity in Northern China. *Environ. Pollut.* **2020**, *262*, 114261. [CrossRef]
10. Yoshida, S.; Hiraga, K.; Takehana, T.; Taniguchi, I.; Yamaji, H.; Maeda, Y.; Toyohara, K.; Miyamoto, K.; Kimura, Y.; Oda, K. A Bacterium That Degrades and Assimilates Poly(Ethylene Terephthalate). *Science* **2016**, *351*, 1196–1199. [CrossRef]
11. Tournier, V.; Topham, C.M.; Gilles, A.; David, B.; Folgoas, C.; Moya-Leclair, E.; Kamionka, E.; Desrousseaux, M.-L.; Texier, H.; Gavalda, S.; et al. An Engineered PET Depolymerase to Break down and Recycle Plastic Bottles. *Nature* **2020**, *580*, 216–219. [CrossRef]
12. Urbanek, A.K.; Rymowicz, W.; Mirończuk, A.M. Degradation of Plastics and Plastic-Degrading Bacteria in Cold Marine Habitats. *Appl. Microbiol. Biotechnol.* **2018**, *102*, 7669–7678. [CrossRef] [PubMed]
13. Li, H.; Luo, Q.; Zhao, S.; Zhao, P.; Yang, X.; Huang, Q.; Su, J. Watershed Urbanization Enhances the Enrichment of Pathogenic Bacteria and Antibiotic Resistance Genes on Microplastics in the Water Environment. *Environ. Pollut.* **2022**, *313*, 120185. [CrossRef] [PubMed]
14. Niu, Y.; An, Z.; Gao, D.; Chen, F.; Zhou, J.; Liu, B.; Qi, L.; Wu, L.; Lin, Z.; Yin, G.; et al. Tidal Dynamics Regulates Potential Coupling of Carbon-nitrogen-sulfur Cycling Microbes in Intertidal Flats. *Sci. Total Environ.* **2023**, *899*, 165663. [CrossRef] [PubMed]
15. Taniguchi, I.; Yoshida, S.; Hiraga, K.; Miyamoto, K.; Kimura, Y.; Oda, K. Biodegradation of PET: Current Status and Application Aspects. *ACS Catal.* **2019**, *9*, 4089–4105. [CrossRef]
16. Fang, C.; He, Y.; Yang, Y.; Fu, B.; Pan, S.; Jiao, F.; Wang, J.; Yang, H. Laboratory Tidal Microcosm Deciphers Responses of Sediment Archaeal and Bacterial Communities to Microplastic Exposure. *J. Hazard. Mater.* **2023**, *458*, 131813. [CrossRef]
17. He, Y.; Fang, C.; Zeng, Z.; Fu, B.; Cui, Z.; Wang, J.; Yang, H. Screening and Isolation of Polyethylene Microplastic Degrading Bacteria from Mangrove Sediments in Southern China. *Sci. Total Environ.* **2025**, *962*, 178488. [CrossRef]
18. Fang, C.; Yang, Y.; Zhang, S.; He, Y.; Pan, S.; Zhou, L.; Wang, J.; Yang, H. Unveiling the Impact of Microplastics with Distinct Polymer Types and Concentrations on Tidal Sediment Microbiome and Nitrogen Cycling. *J. Hazard. Mater.* **2024**, *472*, 134387. [CrossRef]
19. Zhang, X.; Shen, Z.; Wu, J.; Su, M.; Zheng, L.; Xie, M.; Hong, H.; Huang, X.; Lu, H. High Salinity Restrains Microplastic Transport and Increases the Risk of Pollution in Coastal Wetlands. *Water Res.* **2024**, *267*, 122463. [CrossRef]
20. Li, Q.; Huang, Z.; Zhong, Z.; Bian, F.; Zhang, X. Integrated Genomics and Transcriptomics Provide Insights into Salt Stress Response in *Bacillus subtilis* ACP81 from Moso Bamboo Shoot (*Phyllostachys praecox*) Processing Waste. *Microorganisms* **2024**, *12*, 285. [CrossRef]

21. Danso, D.; Chow, J.; Streit, W.R. Plastics: Environmental and Biotechnological Perspectives on Microbial Degradation. *Appl. Environ. Microbiol.* **2019**, *85*, e01095-19. [CrossRef]
22. Chen, S.-Q.; Huang, Q.-S.; Li, Y.; Wu, J.; Chen, S.; Yan, Z.-F. Targeted Aggregation of PETase towards Surface of *Stenotrophomonas pavanii* for Degradation of PET Microplastics. *J. Hazard. Mater.* **2024**, *480*, 135895. [CrossRef]
23. Sun, Y.; Zhang, Y.; Ma, Y.; Xin, R.; Li, X.; Niu, Z. Exploring the Potential of a New Marine Bacterium Associated with Plastisphere to Metabolize Dibutyl Phthalate and Bis(2-Ethylhexyl) Phthalate by Enrichment Cultures Combined with Multi-Omics Analysis. *Environ. Pollut.* **2024**, *342*, 123146. [CrossRef]
24. Sudhakar, M.P.; Hinduja, M.; Sujitha, K.; Kumar, A.G.; Dharani, G. Biodegradation of Seaweed-Based Bioplastics Using Deep-Sea Marine Bacterial Consortia. *Thalassas* **2024**, *40*, 1319–1327. [CrossRef]
25. Xiang, P.; Zhang, Y.; Zhang, T.; Wu, Q.; Zhao, C.; Li, Q. A Novel Bacterial Combination for Efficient Degradation of Polystyrene Microplastics. *J. Hazard. Mater.* **2023**, *458*, 131856. [CrossRef] [PubMed]
26. Li, C.; Wang, L.; Ji, S.; Chang, M.; Wang, L.; Gan, Y.; Liu, J. The Ecology of the Plastisphere: Microbial Composition, Function, Assembly, and Network in the Freshwater and Seawater Ecosystems. *Water Res.* **2021**, *202*, 117428. [CrossRef] [PubMed]
27. Malik, N.; Lakhawat, S.S.; Kumar, V.; Sharma, V.; Bhatti, J.S.; Sharma, P.K. Recent Advances in the Omics-Based Assessment of Microbial Consortia in the Plastisphere Environment: Deciphering the Dynamic Role of Hidden Players. *Process Saf. Environ. Prot.* **2023**, *176*, 207–225. [CrossRef]
28. Yu, X.; Zhang, Y.; Chen, S.; Chen, S.; Wan, C.; Wang, Y.; Zou, L.; Peng, L.; Ye, L.; Li, Q. Study on the Degradation Efficiency and Mechanism of Polystyrene Microplastics by Five Kinds of Edible Fungi. *J. Hazard. Mater.* **2025**, *492*, 138165. [CrossRef]
29. Lang, M.; Yu, X.; Liu, J.; Xia, T.; Wang, T.; Jia, H.; Guo, X. Fenton Aging Significantly Affects the Heavy Metal Adsorption Capacity of Polystyrene Microplastics. *Sci. Total Environ.* **2020**, *722*, 137762. [CrossRef]
30. Auta, H.S.; Emenike, C.U.; Fauziah, S.H. Distribution and Importance of Microplastics in the Marine Environment: A Review of the Sources, Fate, Effects, and Potential Solutions. *Environ. Int.* **2017**, *102*, 165–176. [CrossRef]
31. Caporaso, J.G.; Lauber, C.L.; Walters, W.A.; Berg-Lyons, D.; Huntley, J.; Fierer, N.; Owens, S.M.; Betley, J.; Fraser, L.; Bauer, M.; et al. Ultra-High-Throughput Microbial Community Analysis on the Illumina HiSeq and MiSeq Platforms. *ISME J.* **2012**, *6*, 1621–1624. [CrossRef]
32. Bolyen, E.; Rideout, J.R.; Dillon, M.R.; Bokulich, N.A.; Abnet, C.C.; Al-Ghalith, G.A.; Alexander, H.; Alm, E.J.; Arumugam, M.; Asnicar, F.; et al. Reproducible, Interactive, Scalable and Extensible Microbiome Data Science Using QIIME 2. *Nat. Biotechnol.* **2019**, *37*, 852–857. [CrossRef] [PubMed]
33. Wang, L.; Luo, Z.; Zhen, Z.; Yan, Y.; Yan, C.; Ma, X.; Sun, L.; Wang, M.; Zhou, X.; Hu, A. Bacterial Community Colonization on Tire Microplastics in Typical Urban Water Environments and Associated Impacting Factors. *Environ. Pollut.* **2020**, *265*, 114922. [CrossRef] [PubMed]
34. Xiang, Y.; Zhu, A.; Guo, Y.; Liu, G.; Chen, B.; He, B.; Liang, Y.; Yin, Y.; Cai, Y.; Jiang, G. Decreased Bioavailability of Both Inorganic Mercury and Methylmercury in Anaerobic Sediments by Sorption on Iron Sulfide Nanoparticles. *J. Hazard. Mater.* **2022**, *424*, 127399. [CrossRef]
35. Maheswaran, B.; Al-Ansari, M.; Al-Humaid, L.; Sebastin Raj, J.; Kim, W.; Karmegam, N.; Mohamed Rafi, K. *In Vivo* Degradation of Polyethylene Terephthalate Using Microbial Isolates from Plastic Polluted Environment. *Chemosphere* **2023**, *310*, 136757. [CrossRef]
36. Rong, Z.; Xu, X.-W.; Wu, Y.-H. Biodegradation of Low-Density Polyethylene Film by Two Bacteria Isolated from Plastic Debris in Coastal Beach. *Ecotoxicol. Environ. Saf.* **2024**, *278*, 116445. [CrossRef] [PubMed]
37. Kavitha, R.; Bhuvaneswari, V. Assessment of Polyethylene Degradation by Biosurfactant Producing Ligninolytic Bacterium. *Biodegradation* **2021**, *32*, 531–549. [CrossRef]
38. Roager, L.; Sonnenschein, E.C. Bacterial Candidates for Colonization and Degradation of Marine Plastic Debris. *Environ. Sci. Technol.* **2019**, *53*, 11636–11643. [CrossRef]
39. Giyahchi, M.; Moghimi, H. Sustainable Solution for Microplastic Removal: Sequential Biodegradation and Detoxification of Polyethylene Terephthalate Microplastics by Two Natural Microbial Consortia. *Ecotoxicol. Environ. Saf.* **2025**, *302*, 118738. [CrossRef]
40. Li, S.; Liu, J.; Su, L.; Qiu, J.; Lin, L.; Kovács, Á.T.; Lin, Y. Synergistic Biodegradation of Polyethylene by Experimentally Evolved Bacterial Biofilms. *ISME J.* **2025**, *19*, wraf223. [CrossRef]
41. Roberts, C.; Edwards, S.; Vague, M.; León-Zayas, R.; Scheffer, H.; Chan, G.; Swartz, N.A.; Mellies, J.L. Environmental Consortium Containing *Pseudomonas* and *Bacillus* Species Synergistically Degrades Polyethylene Terephthalate Plastic. *mSphere* **2020**, *5*, 1–20. [CrossRef]
42. Benavides Fernández, C.D.; Guzmán Castillo, M.P.; Quijano Pérez, S.A.; Carvajal Rodríguez, L.V. Microbial Degradation of Polyethylene Terephthalate: A Systematic Review. *SN Appl. Sci.* **2022**, *4*, 263. [CrossRef]
43. Oberbeckmann, S.; Labrenz, M. Marine Microbial Assemblages on Microplastics: Diversity, Adaptation, and Role in Degradation. *Annu. Rev. Mar. Sci.* **2020**, *12*, 209–232. [CrossRef]

44. Lear, G.; Kingsbury, J.M.; Franchini, S.; Gambarini, V.; Maday, S.D.M.; Wallbank, J.A.; Weaver, L.; Pantos, O. Plastics and the Microbiome: Impacts and Solutions. *Environ. Microbiome* **2021**, *16*, 2. [CrossRef]
45. Wei, R.; Zimmermann, W. Microbial Enzymes for the Recycling of Recalcitrant Petroleum-Based Plastics: How Far Are We? *Microb. Biotechnol.* **2017**, *10*, 1308–1322. [CrossRef]
46. Gewert, B.; Plassmann, M.M.; MacLeod, M. Pathways for Degradation of Plastic Polymers Floating in the Marine Environment. *Environ. Sci. Process. Impacts* **2015**, *17*, 1513–1521. [CrossRef]
47. Zettler, E.R.; Mincer, T.J.; Amaral-Zettler, L.A. Life in the "Plastisphere": Microbial Communities on Plastic Marine Debris. *Environ. Sci. Technol.* **2013**, *47*, 7137–7146. [CrossRef]
48. Amaral-Zettler, L.A.; Zettler, E.R.; Mincer, T.J. Ecology of the Plastisphere. *Nat. Rev. Microbiol.* **2020**, *18*, 139–151. [CrossRef] [PubMed]
49. Bhagwat, G.; Zhu, Q.; O'Connor, W.; Subashchandrabose, S.; Grainge, I.; Knight, R.; Palanisami, T. Exploring the Composition and Functions of Plastic Microbiome Using Whole-Genome Sequencing. *Environ. Sci. Technol.* **2021**, *55*, 4899–4913. [CrossRef]
50. Pinto, M.; Polania Zenner, P.; Langer, T.M.; Harrison, J.; Simon, M.; Varela, M.M.; Herndl, G.J. Putative Degraders of Low-density Polyethylene-derived Compounds Are Ubiquitous Members of Plastic-associated Bacterial Communities in the Marine Environment. *Environ. Microbiol.* **2020**, *22*, 4779–4793. [CrossRef] [PubMed]
51. Ogonowski, M.; Motiei, A.; Ininbergs, K.; Hell, E.; Gerdes, Z.; Udekwu, K.I.; Bacsik, Z.; Gorokhova, E. Evidence for Selective Bacterial Community Structuring on Microplastics. *Environ. Microbiol.* **2018**, *20*, 2796–2808. [CrossRef] [PubMed]
52. Sushmitha, T.J.; Rajeev, M.; Sriyutha Murthy, P.; Ganesh, S.; Toleti, S.R.; Karutha Pandian, S. Bacterial Community Structure of Early-Stage Biofilms Is Dictated by Temporal Succession Rather than Substrate Types in the Southern Coastal Seawater of India. *PLoS ONE* **2021**, *16*, e0257961. [CrossRef]
53. Kim, S.Y.; Lee, S.-W.; Lee, E.-H. Growth and Membrane Stress Responses in *E. coli* and *Acinetobacter* sp. upon Exposure to Functionalized Polystyrene Microplastics. *Environ. Anal. Health Toxicol.* **2025**, *40*, e2025017. [CrossRef]
54. Wright, R.J.; Erni-Cassola, G.; Zadjelovic, V.; Latva, M.; Christie-Oleza, J.A. Marine Plastic Debris: A New Surface for Microbial Colonization. *Environ. Sci. Technol.* **2020**, *54*, 11657–11672. [CrossRef]
55. Nadeau, L.J.; Barlow, D.E.; Hung, C.-S.; Biffinger, J.C.; Crouch, A.L.; Hollomon, J.M.; Ecker, C.D.; Russell, J.N.; Crookes-Goodson, W.J. Colonization and Degradation of Polyurethane Coatings by *Pseudomonas protegens* Biofilms Is Promoted by PueA and PueB Hydrolases. *Int. Biodeterior. Biodegrad.* **2021**, *156*, 105121. [CrossRef]
56. Mann, E.E.; Wozniak, D.J. Pseudomonas Biofilm Matrix Composition and Niche Biology. *FEMS Microbiol. Rev.* **2012**, *36*, 893–916. [CrossRef]
57. Ameen, F.; Al-Shwaiman, H.A.; Almalki, R.; Al-Sabri, A.E.; Sholkamy, E.N. Degradation of Polyvinyl Chloride (PVC) Microplastics Employing the Actinobacterial Strain *Streptomyces gobitricini*. *Biodegradation* **2025**, *36*, 19. [CrossRef] [PubMed]
58. Hakkarainen, M.; Albertsson, A.-C. Environmental Degradation of Polyethylene. In *Long Term Properties of Polyolefins*; Albertsson, A.-C., Ed.; Springer: Berlin/Heidelberg, Germany, 2004; pp. 177–200, ISBN 978-3-540-45196-9.
59. Craft, C.; Broome, S.; Campbell, C. Fifteen Years of Vegetation and Soil Development after Brackish-Water Marsh Creation. *Restor. Ecol.* **2002**, *10*, 248–258. [CrossRef]
60. Cheng, C.; Li, F. Ecosystem Restoration and Management Based on Nature-Based Solutions in China: Research Progress and Representative Practices. *Nat.-Based Solut.* **2024**, *6*, 100176. [CrossRef]

Disclaimer/Publisher's Note: The statements, opinions and data contained in all publications are solely those of the individual author(s) and contributor(s) and not of MDPI and/or the editor(s). MDPI and/or the editor(s) disclaim responsibility for any injury to people or property resulting from any ideas, methods, instructions or products referred to in the content.